Circumstellar effects on the chemical abundances in AGB stars

O. Zamora[1,2]

[1] Instituto de Astrofísica de Canarias (IAC), E-38200 La Laguna, Tenerife, Spain
[2] Departamento de Astrofísica, Universidad de La Laguna (ULL), E-38206 La Laguna, Tenerife, Spain, e-mail: `ozamora@iac.es`

Abstract. In this work we explore how the use of dynamical model atmospheres has an impact on the chemical abundances derived in O-rich (massive) AGB stars. In particular, we study the effect on the Rb and Zr abundances derived from the resonant 7800 Å Rb I line and the 6474 Å ZrO bandhead, respectively. Interestingly, our new Rb abundances, including a stellar wind, are much lower (by 1-2 dex) in those O-rich AGB stars showing the higher circumstellar expansion velocities, while the new Zr abundances remain close to the solar values. The Rb and Zr derived here significantly resolve the problem of the present mismatch between the observations of intermediate-mass (4–8 $M_\odot$) Rb-rich AGB stars and the AGB nucleosynthesis theoretical predictions.

Key words. Stars: abundances – Stars: atmospheres

1. Introduction

The asymptotic giant branch (AGB) is the last nuclear-burning phase of low- and intermediate-mass stars ($0.8 \leq M \leq 8\ M_\odot$), where the production of heavy elements ($Z > 26$) by *slow* neutron-captures (the *s*-process) on iron seed nuclei takes place. The relative abundance of s-elements such as Rb to other neighboring ones such as Sr, Y, and Zr is an indicator of the neutron density, namely a discriminant of the stellar mass and the main neutron source at the *s*-process site (Lambert et al. 1995; Abia et al. 2001; García-Hernández et al. 2006).

Low-mass AGB stars ($M < 4\ M_\odot$) can turn C-rich (i.e. C/O > 1) because of the dredge-up of carbon from the bottom of the convective envelope to the stellar surface. The ^{13}C(α, n)^{16}O reaction is accepted to operate as the main neutron source (e.g. Abia et al. 2001) in these stars. On the other hand, intermediate-mass AGB stars ($4 \leq M \leq 8\ M_\odot$) are O-rich stars (C/O < 1) because of the operation of hot bottom burning (HBB), which burns carbon at the base of the convective envelope, thus preventing the formation of a carbon star (Sackmann & Boothroyd 1992). The *s*-process elements are expected to form mainly by the neutrons released by the ^{22}Ne(α, n)^{25}Mg reaction, in a higher neutron density environment than in lower mass AGB stars (García-Hernández et al. 2006). Observationally, intermediate-mass AGB stars display [Rb/Zr] > 0 (García-Hernández et al. 2006, 2007, 2009) while low-mass AGB stars have [Rb/Zr] < 0 ratios (Abia et al. 2001).
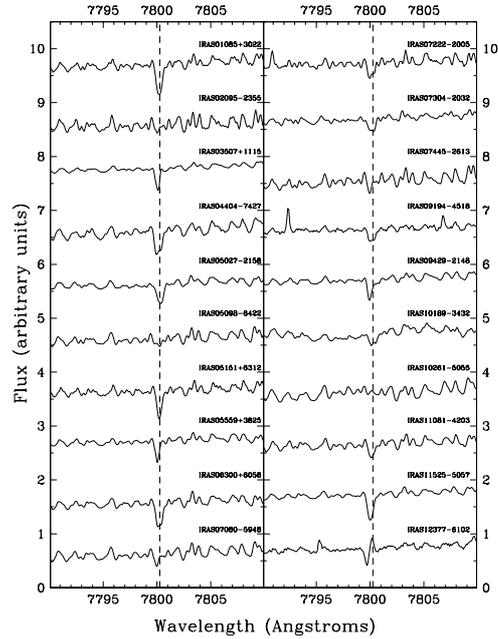
However, the Rb abundances and [Rb/Zr] ratios found in several Galactic and Magellanic

Cloud intermediate-mass AGB stars (García-Hernández et al. 2006, 2009) represent a challenge for theoretical AGB nucleosynthesis models, which do not predict the extreme Rb over-abundances ([Rb/Fe] $\gtrsim$ 2 dex) and extraordinarily high [Rb/Zr] ratios observed (van Raai et al. 2012; Karakas et al. 2012). These Rb abundances were derived from the resonant Rb I absorption line at 7800 Å, using hydrostatic model atmospheres. The detection of blue-shifted circumstellar (CS) Rb I absorption lines in several of these extreme O-rich AGB stars suggests that the Rb I line is probably affected by contamination from one or more CS components. In this work, we explore how the use of a more realist model atmosphere (including a stellar wind) impact the Rb and Zr chemical abundances derived in intermediate-mass AGB stars.

Fig. 1. Observed Rb line profiles in several Galactic OH/IR AGB stars (García-Hernández et al. 2006). The location of the Rb I (7800.3 Å) line is indicated by the dashed line.

2. Methodology

2.1. Spectral synthesis including velocity fields

The circumstellar component around the Rb I 7800 Å line was modeled using a branch of the v12.1 of the spectral synthesis code *Turbospectrum* (Alvarez & Plez 1998; Plez & Lambert 2002) that is able to deal with extended atmospheres and velocity fields. The Doppler effect due to the expanding envelope of the star is implemented in *Turbospectrum* by the modification of the routines that compute the line intensities at the stellar surface (see Zamora et al. 2014, for further details). As an independent test of consistency, Monte Carlo (MCS) simulations were also carried out in order to validate the results obtained by *Turbospectrum*. The most frequent line profile obtained from MCS is a blue-shifted absorption feature with a weak and broader emission component. This is in agreement with the optical observations of the Rb line profile obtained by García-Hernández et al. (2006) in Galactic OH/IR AGB stars; see also Figure 1 .

2.2. Dynamical model atmospheres

The dynamical models are constructed from the original MARCS hydrostatic atmosphere model structure, expanding the atmosphere radius by the inclusion of a wind out to ~ 5 stellar radii, with a radial velocity field in spherical symmetry. The stellar radius R_* is defined as the radius corresponding to $r(\tau_{Ross} = 1)$ in the MARCS hydrostatic model, where r is the distance from the stellar centre and τ_{Ross} the Rosseland optical depth. The stellar wind is computed under the assumptions of mass conservation and radiative thermal equilibrium following a classical β−velocity law (see Eqs. 1-3 in Zamora et al. 2014).

The β exponent is an arbitrary free parameter controlling the slope of the β−velocity law. For the onset of the wind, we take $v_0 = v(R_*)$ and the extension of the envelope begins from the outer radius of the hydrostatic model. For

the mass-loss rate $\dot{M}$ and the β exponent, we use values in the typical range of AGB stars: $\dot{M} \sim 10^{-9}$–10^{-4} M$_\odot$ yr^{-1} in steps of factors of 10 and $\beta \sim 0$–1.6 in steps of 0.2. Finally, we assume $v_{exp}(OH)$ as the terminal velocity v_∞ because the OH maser emission is found at very large distances of the central star (see e.g. Decin et al. 2010).

3. Comparison between hydrostatic and dynamical Rb and Zr abundances

The parameters of the dynamical atmosphere models providing the best fit to the observations and the derived Rb and Zr abundances ([Rb/M]$_{dyn}$ and [Zr/M]$_{dyn}$) are shown in Table 1. The Rb abundances ([Rb/M]$_{static}^{ref}$) as determined from hydrostatic models by García-Hernández et al. (2006, 2009) are also shown for comparison. In Table 1 we also lists the re-derived Rb abundances ([Rb/M]$_{static}$) using the hydrostatic models with the updated solar abundances by Grevesse et al. (2007).

The new Rb abundances (in the range [Rb/M]$\sim$0.0−1.5 dex; Table 1) derived from our dynamical models display a dramatic decrease of 1.4 dex to 1.8 dex with respect to the static case. For the less extreme stars with a lower expansion velocity and mass-loss rate (IRAS 05098−6422 and IRAS 18429−1721), the Rb abundances obtained from dynamical models remain close, within 0.2 dex, to those from hydrostatic models.

In Fig. 2, we display the observed Rb I line profiles in our O-rich AGB sample (black dots) together with the best synthetic spectra as obtained from the new dynamical models (red lines) versus the static ones (blue lines). Our dynamical atmosphere models reproduce the observed Rb I line profiles (photospheric and circumstellar components) very well, much better than the classical hydrostatic models. The 6474 Å ZrO bandhead, because it is formed deeper in the atmosphere, is less affected than the Rb I line, and the Zr abundances derived from dynamical models are similar to those obtained with the hydrostatic models.

Standard nucleosynthesis models for intermediate-mass AGB stars show that
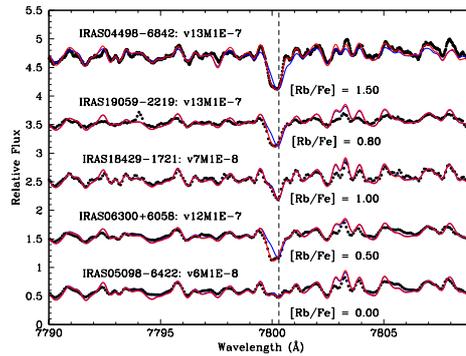
Fig. 2. Rb abundances derived in the sample stars using dynamical models. The location of the Rb I stellar line is indicated by a dashed line. Dynamical models providing the best fits to the observations (black dots) are indicated by a red line. Hydrostatic models are also shown for comparison (blue lines). The expansion velocity and the mass-loss rate adopted in the models also are indicated for each star.

the predicted Rb abundances range from [Rb/M]$\sim$0.0 up to 1.44 dex, depending on the progenitor mass and metallicity (see van Raai et al. 2012; Karakas et al. 2012); the predicted Rb production increases with increasing stellar mass and decreasing metallicity. Comparing with their predictions, the Rb abundances and [Rb/Zr] ratios derived here significantly resolve the problem of the present mismatch between the observations of massive (4–8 M$_\odot$) Rb-rich AGB stars and the theoretical predictions.

4. Conclusions

We explore the CS effects on the Rb and Zr abundances derived in extreme O-rich AGB stars. To this end, we use more realistic model atmospheres that include a gaseous CS envelope. The much lower Rb abundances (and [Rb/Zr] ratios) derived here significantly alleviate the actual mismatch between the AGB nucleosynthesis predictions and the optical observations of intermediate-mass (4–8 M$_\odot$) Rb-rich AGB stars. Further work is been doing in order to carry out a chemical analysis based

Table 1. Atmosphere parameters and abundances derived using dynamical models vs. hydrostatic models.

IRAS name	$T_{\rm eff}$ (K)	log g	β	$\dot{M}$ (M$_\odot$ yr^{-1})	v (km s^{-1})	[Rb/M]$_{static}^{ref\,a}$	[Rb/M]$_{static}{}^{b}$	[Rb/M]$_{dyn}{}^{b}$	[Zr/M]$_{dyn}{}^{b}$
Galactic stars									
05098−6422	3000	−0.5	0.2	1.0×10^{-8}	6	0.1	0.0 ± 0.4	0.0 ± 0.4	≤ 0.3 ± 0.3
06300+6058	3000	−0.5	0.2	1.0×10^{-7}	12	1.6	1.9 ± 0.4	0.5 ± 0.7	≤ 0.1 ± 0.3
18429−1721	3000	−0.5	0.2	1.0×10^{-8}	7	1.2	1.2 ± 0.4	1.0 ± 0.4	≤ 0.3 ± 0.3
19059−2219	3000	−0.5	0.2	1.0×10^{-7}	13	2.3/2.6	2.4 ± 0.4	0.8 ± 0.7	≤ 0.3 ± 0.3
LMC star									
04498−6842	3400	0.0	0.2	1.0×10^{-7}	13	3.9^{c}	3.3 ± 0.4	1.5 ± 0.7	≤ 0.3 ± 0.3

[a] See García-Hernández et al. (2006, 2009). [b] The uncertainties represent the formal errors due to the sensitivity of the derived abundances to slight changes in the model atmosphere parameters (ΔT_{eff}=±100 K, Δ[M/H]=±0.3, $\Delta\,\xi$=±1 kms^{-1}, Δlog g=+0.5, ΔFWHM=50 mÅ, $\Delta\beta$=0.2, Δlog($\dot{M}$/M$_\odot$yr^{-1})=1.0 for each star. [c] We scale the Rb overabundance derived by García-Hernández et al. (2009), [Rb/M] = +5.0, to the adopted LMC metallicity [M/H] = −0.3.

on these new dynamical models for all the Rb-rich AGB stars already studied by García-Hernández et al. (2006, 2009). This undoubtedly will help us to constrain the actual nucleosynthesis models for the more massive AGB stars.

References

Abia, C., Busso, M., Gallino, R., et al. 2001, ApJ, 559, 1117

Alvarez, R., & Plez, B. 1998, A&A, 330, 1109

Decin, L., Justtanont, K., De Beck, E., et al. 2010, A&A, 521, L4

García-Hernández, D. A., García-Lario, P., Plez, B., et al. 2006, Science, 314, 1751

García-Hernández, D. A., García-Lario, P., Plez, B., et al. 2007, A&A, 462, 711

García-Hernández, D. A., Manchado, A., Lambert, D. L., et al. 2009, ApJ, 705, L31

Grevesse, N., Asplund, M., & Sauval, A. J. 2007, Space Sci. Rev., 130, 105

Karakas, A. I., García-Hernández, D. A., & Lugaro, M. 2012, ApJ, 751, 8

Lambert, D. L., et al. 1995, ApJ, 450, 302

Plez, B., & Lambert, D. L. 2002, A&A, 386, 1009

Sackmann, I.-J., & Boothroyd, A. I. 1992, ApJ, 392, L71

van Raai, M. A., et al., & Yong, D. 2012, A&A, 540, A44

Zamora, O., et al. 2014, A&A, 564, L4